TEN: Twin Embedding Networks for the Jigsaw Puzzle Problem with Eroded Boundaries

Daniel Rika

Dept. of Computer Science Bar-Ilan University Israel, Ramat-Gan 52900 danielrika@gmail.com

Dror Sholomon

Dept. of Computer Science Bar-Ilan University Israel, Ramat-Gan 52900 dror.sholomon@gmail.com

Nathan S. Netanyahu

Dept. of Computer Science Bar-Ilan University Israel, Ramat-Gan 52900 nathan@cs.biu.ac.il

Eli (Omid) David

Dept. of Computer Science Bar-Ilan University Israel, Ramat-Gan 52900 mail@elidavid.com

ABSTRACT

The *jigsaw puzzle problem* (JPP) is a well-known research problem, which has been studied for many years. Solving this problem typically involves a two-stage scheme, consisting of the computation of a pairwise piece compatibility measure (CM), coupled with a subsequent puzzle reconstruction algorithm. Many effective CMs, which apply a simple distance measure, based merely on the information along the piece edges, have been proposed. However, the practicality of these classical methods is rather doubtful for problem instances harder than pure synthetic images. Specifically, these methods tend to break down in more realistic scenarios involving, e.g., monochromatic puzzles, eroded boundaries due to piece degradation over long time periods, missing pieces, etc. To overcome this significant deficiency, a few deep convolutional neural network (CNN)-based CMs have been recently introduced. Despite their promising accuracy, these models are very computationally intensive. We introduce in this paper, for the first time, a powerful CNN architecture, called Twin Embedding Networks (TEN), to represent a piece with respect to its boundary in a latent embedding space. Combining this latent representation with a simple distance measure, we then demonstrate a superior performance, in terms of accuracy, of our newly proposed pairwise CM, compared to that of various classical methods, for the problem domain of *eroded tile boundaries*, a testbed for a number of real-world JPP variants. Furthermore, we also demonstrate that TEN is faster by a few orders of magnitude, on average, than the recent NN models, i.e., it is as fast as the classical methods. In this regard, the paper makes a significant first attempt at bridging the gap between the relatively low accuracy (of classical methods) and the intensive computational complexity (of NN models), for practical, real-world puzzle-like problems.

1 Introduction

Numerous successful studies have been pursued over the years for solving the intriguing *jigsaw puzzle problem* (JPP). In particular, most advanced methods have focused recently on jigsaw puzzles containing non-overlapping square pieces. The reconstruction of such puzzles is composed typically of two main steps. First, a *compatibility measure* (CM) is computed for all pairwise piece sides, to obtain numerically the degree of compatibility for each possible piece pair. After computing all of the pairwise CMs, a reconstruction phase kicks in. The goal of any reconstruction algorithm is to determine correctly the location and orientation of each piece. relying solely on the CM scores computed in the first step. All previous works vary in the way they compute the pairwise CMs and in the way they try to assemble a puzzle as accurately as possible. Although the two steps are equally essential for the reconstruction, we focus here on the CM

computation of all pairwise pieces, which could be highly expensive due to the order of $\mathcal{O}(N^2)$ operations required. (Note that an N-piece puzzle requires $16N^2$ pairwise CM computations.)

Classical, most commonly used CMs include the *sum of squared distances* (SSD) proposed by Cho *et al.* [1], the so-called *prediction-based compatibility* (employing $(L_p)^q$ variants) proposed by Pomerantz *et al.* [2], the L_1 -norm compatibility of Paikin and Tal [3], and the *Mahalanobis gradient compatibility* (MGC) proposed by Gallagher [4]. These and other measures (*e.g.* [5, 6, 7]) yield high quality CMs, which allow for successful reconstruction of very large puzzles with up to tens of thousands of pieces.

The effectiveness of the above methods greatly depends, however, on the notion of a *synthetic puzzle*, *i.e.* a puzzle obtained by cropping a high-resolution image into N non-overlapping square pieces of size $P \times P$ pixels. (Such puzzles contain perfect pieces, and are considered information rich.) Indeed, the classical methods tend to be simple, fast, and very accurate under this favorable working assumption, which bodes well with CMs based mostly on piece boundary pixels.

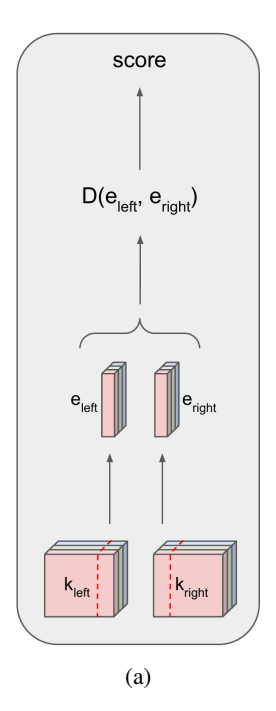
When encountering, though, harder puzzle problems (due to various *real-world* scenarios, such as monochromatic puzzles, eroded piece boundaries, missing pieces, etc.), the classical measures tend to perform poorly, thereby affecting negatively the reconstruction outcome. Mondal *et al.* [8] were the first to handle this weak spot for puzzles containing *eroded boundaries*. They proposed a new pairwise CM called weighted-MGC (wMGC), which combines the SSD and MGC CMs. Despite their slight improvement, their wMGC still suffers from severe degradation in performance for eroded piece boundaries of 1–2 pixels.

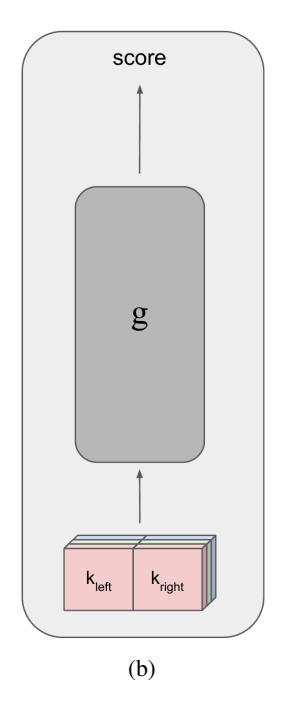
The growing influence of *deep neural networks* (DNNs), in many related fields, has given rise recently also to the development of more accurate and robust CMs for harder variants of the JPP. Pai \tilde{x} ao *et al.* [9] used a pre-trained SqueezeNet [10] model and fine-tuned it to obtain an effective CM for *strip-cut shredded documents*. Their NN-based pairwise CM enabled them to reassemble mechanically shredded documents with 94% accuracy. Another real-world JPP variant concerns the reconstruction of *Portuguese tile panels*, where often (square) real panel tiles have been severely degraded chromatically and eroded along their edges over hundreds of years. Rika *et al.* [11] proposed an ensemble of four NN-based models for dealing with this challenging variant. Their NN-based CM provides a significant improvement over classical methods, which made the reconstruction of Portuguese panels feasible for the first time. Regarding the problem of eroded boundaries, Bridger *et al.* [12] used a *generative adversarial network* (GAN) to "in-paint" the gap between pairs of pieces. After sufficient training of their generator, they keep its weights fixed and apply a second training stage to fine-tune the discriminator to differentiate between a true adjacent in-paint pair and false ones. Inspired by Pix2Pix [13], their generator uses a U-Net encoder-decoder architecture [14] and a Markovian discriminator with a 3-layer encoder. They carried out their work on a piece size 64×64 pixels, with an erosion of 2 or 4 boundary pixels, and reported superior results to those of the classical L_1 -norm compatibility. Other methods aimed at solving the JPP entirely by DNNs [15, 16] were shown to work only on virtually impractical puzzle sizes of 4×4 .

Unfortunately, NN-based CMs consist of millions of parameters, such that each inference becomes very computationally-intensive. Since the model should be employed $16N^2$ times for an N-piece puzzle, the entire CM phase becomes highly infeasible in the lack of powerful dedicated hardware. To alleviate significantly this serious deficiency, we propose in this paper a new methodology for computing efficiently a pairwise CM via $Twin\ Embedding\ (Neural)\ Networks$ called TEN. The main idea of our novel approach is to employ these networks to represent an $entire\ puzzle\ piece$ with respect to $each\ of\ its\ boundaries\ in\ a\ latent\ embedding\ space$. Combining this representation with a simple distance measure, we then demonstrate that our newly obtained CM is significantly more accurate than well-known classical CMs and, at the same time, is faster by a few orders of magnitude than typical NN-based CMs. The main highlights of our work are summarized as follows:

- Proposed a new NN-based framework and architecture to represent via embeddings an entire puzzle piece with respect to its boundaries;
- Demonstrated how to use embedding neural networks to speedup regular end-to-end NN-based scheme by a few orders of magnitude;
- Presented extensive Top-1 accuracy and reconstruction results, which demonstrate TEN's superior performance to most classical CMs.
- Conducted extensive tests on 100 eroded puzzles of roughly a thousand pieces each, to further establish the
 advantageous performance of our proposed framework relatively to previous CM methods.

We believe that the above contributions make a significant first step at bridging the gap between the relative low accuracy (of classical CMs) and the intensive computational complexity (of NN-based models), for various real-world puzzle-like problems.





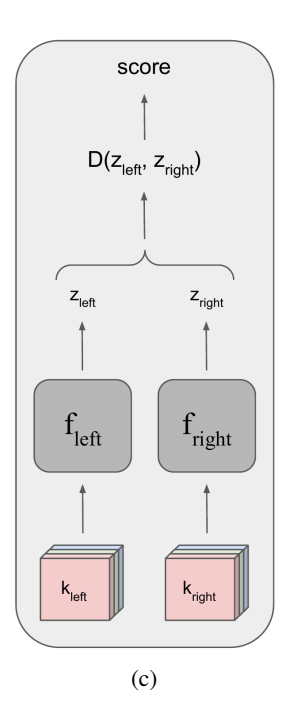


Figure 1: Schematic architectures of (a) traditional, (b) NN-based, and (c) TEN for CM computation. Note that *D* represents a general distance measure function (not necessarily the same in (a) and (c)).

The rest of the paper is organized as follows. Section 2 describes in detail TEN's framework and architecture. Section 3 presents our extensive experimental results, including a comparative performance evaluation with previous classical CMs. Finally, Section 4 makes concluding remarks and discusses future work.

2 TEN: Twin Embedding (Neural) Networks

Traditional methods (not based on NN models) typically compute the distance measure, $D(e_l,e_r):\mathbb{R}^d\times\mathbb{R}^d\to\mathbb{R}$, for computing the CM of a given pair of tiles, where e_l and e_r correspond, respectively, to the pixels along the left and right tile edges. Initially, only edge pixels were usually taken into account. More recent methods (like Gallagher's MGC) considered 2-pixel wide edges for more informative processing. Hence, if a puzzle contains $P\times P\times C$ -size pieces, where P and C denote, respectively, the piece dimensions and number of (color) channels, then $e_l, e_r \in \mathbb{R}^{P\times 2\times C}$. In contrast, NN-based dissimilarity functions work directly on an *entire tile pair* $[k_l:k_r]$, in an attempt to exploit maximum content information from the pieces k_l and k_r , which can be formulated as $g([k_l:k_r]):\mathbb{R}^{P\times 2P\times C}\to\mathbb{R}$. Thus, the computational complexity associated with these functions is considerably more intensive.

Instead, we propose a hybrid approach, which uses an NN-based model for extracting the semantic information of a piece k into a latent space \mathcal{Z} , and combining it with a relatively simple distance measure D, to determine how two latent vectors are compatible to each other. The idea is that the NN-based model $f: \mathbb{R}^{P \times P \times C} \to \mathbb{R}^d$ extracts, in this manner, the most relevant features of the entire piece content with respect to each of its edges. Obviously, we would need two networks to obtain the above representations for a given pair of pieces, *i.e.* a left network f_{left} and a right network f_{right} for the left piece and right piece, respectively. Similarly to the traditional CM computations of a given pair, which work on edge pixels, we can now apply simply a distance measure $D(z_l, z_r): \mathcal{Z} \times \mathcal{Z} \to \mathbb{R}$ with respect to the latent representations $z_l = f_{left}(k_l)$ and $z_r = f_{right}(k_r)$ of the pieces. (Note, that physically z_l corresponds to the right edge of k_l , and z_r corresponds to the left edge of k_r .) In our case, the dimensionality of the latent space is (expected to be) much smaller than that of the traditional approaches, as these methods operate on (all of) the raw edge pixels. See Figure 1 for the different schematic architectures of the above main approaches.

2.1 Architecture

As indicated before, TEN consists of twin CNN-based models, sharing the same architecture but with different learned weights. Each twin network of our small version of TEN consists of four convolutional layers and two interleaving

max-pooling layers [17], using non-linear ReLu activation layers [18], and a fully-connected layer on top to project the CNN's outputs onto an embedding vector in \mathbb{Z} . See Table 1 below for a detailed architecture.

Table 1: Our core architecture of both f_{left} and f_{right} embedding models; total number of model parameters depends on piece size and embedding dimension, *i.e.* (28, 28, 3) and d = 40, in our case; training our NN-based E2E model was done with input size of (28, 56, 3) and d = 1.

Layer Type	Output Dim	# Params
Input	(H, W, 3)	-
Conv2D, filter=(3, 3)	(H, W, 64)	1,728
Conv2D, filter=(3, 3)	(H, W, 128)	73,728
MaxPool2D, filter=(2, 2)	(H/2, W/2, 128)	-
Conv2D, filter=(3, 3)	(H/2, W/2, 256)	294,912
MaxPool2D, filter=(2, 2)	(H/4, W/4, 256)	-
Conv2D, filter=(3, 3)	(H/4, W/4, 512)	1,179,648
Linear	(d,)	32HWd
Total parameters:	1,550,016 + 32HWd	

To extract even higher-quality embedding vectors, we also propose a larger version TEN-Large, in which each twin is an ensemble of four CNN-based networks with the same architecture as in Table 1, but with different inputs. Following [11], each sub-network receives a unique color channel (*i.e.* red, green or blue), and the fourth network receives the entire (3-channel) RGB input. TEN-Large has 20.4M parameters, *i.e.* 4 times as many as the the original TEN, as well as 4 times the number of embeddings. The pairwise compatibility using TEN-Large is given by

$$CM_{\text{TEN-Large}}(k_l, k_r) = \frac{1}{4} \sum_{i} D(f_{left}^i(k_l), f_{right}^i(k_r)), \tag{1}$$

where i represents a sub-network index of the ensemble.

2.2 Training with Embeddings

A procedure for computing a pairwise CM should return the lowest distance between an *anchor* boundary and its true adjacent piece boundary (*i.e. positive pair*), relatively to the distances between the *anchor* boundary and any piece edge in the puzzle (*i.e. negative pairs*). In order to train our twin embedding networks to do so, we used *triplet-loss* [19] defined by the following objective function:

$$\mathcal{L}_{triplet} = \max(0, D(z_a, z_p) - D(z_a, z_n) + \gamma), \tag{2}$$

where γ is set to 1, z_a denotes the embedding vector of f_{left} (as the anchor edge is always located on the left-hand side), and where z_p and z_n denote the embedding vectors of f_{right} (for the positive and negative edges, respectively), as they are located on the right-hand side. Plausible distance measures could be the inverse cosine similarity, L_1 distance, Euclidean distance, or any other distance measure between two vectors. In principle, we found that picking triplet piece edges from the same puzzle leads to better performance. This could be attributed to the notion that negative piece edges from the same puzzle are more likely to be similar to their positive counterparts, thereby forcing the twin embedding networks to extract more discriminative embedding vectors.

2.3 Post Processing

Note that TEN will return different dissimilarity scores for a given pair and its rotated version by 180° , since these pairs do not look the same from the network's perspective. Of course, obtaining an asymmetric compatibility measure for the very same pair does not make sense. To remedy this undesired effect, we apply post processing after computing all pairwise permutations (k_i, k_j) . First, we normalize the compatibility measure with respect to a specific piece edge to be in the range between 0 to 1 as follows:

$$CM'(k_i, k_j) = \frac{CM(k_i, k_j) - min(CM(k_i, *))}{max(CM(k_i, *)) - min(CM(k_i, *))}$$
(3)

We then ensure symmetry for the same pair of pieces by defining:

$$CM''(k_i, k_j) = CM''(k_j, k_i) = \frac{CM'(k_i, k_j) + CM'(k_j, k_i)}{2}$$
(4)

2.4 Type-1 and Type-2 Puzzles

It is common to consider the JPP at two levels of difficulties, namely $\mathit{Type-1}$ and $\mathit{Type-2}$. Type-1 assumes that only piece locations are unknown, while their orientations are fixed and known. Type-2 relaxes this assumption, i.e. piece orientations are also unknown. Note that a CM for Type-1 needs to discriminate, for each anchor piece k_a , between its positive piece k_p (i.e. ground-truth neighbor) and all of the negative candidates k_n , from a total number of N-1 candidates. For Type-2, the total number of candidates rises to 4(N-1), as there are 4 possible orientations for each piece. From a combinatorial point of view, there are essentially 4N anchor edges for an N-piece puzzle, such that each anchor edge has N-1 and 4(N-1) possible matching edges, for Type-1 and Type-2, respectively. In other words, a CM needs to be computed 4N(N-1) and 16N(N-1) times, i.e. roughly $4N^2$ and $16N^2$ times for Type-1 and Type-2, respectively.

2.5 Fast Inference

Let us now examine theoretically the significant reduction in time complexity due to the use of embeddings, as described in Section 2. Assume a puzzle of N pieces with unknown piece position and orientation. As previously indicated, there are $16N^2$ possible combinations for this Type-2 variant, *i.e.* a CM module must be executed for all of these $16N^2$ combinations. Computing CMs for this large number of combinations by the classical methods may not have been a major issue, due to their relatively simple computation. In contrast, NN-based CMs are very computationally intensive, which makes them rather slow and virtually impractical for puzzles containing more than a few hundred pieces. Fortunately, our proposed TEN framework offers a highly-efficient alternative. Observe that each of the f_{left} and f_{right} networks needs to execute only 4N times to capture all of the 4-edge representations of each puzzle piece. After TEN is executed 4N times, we save all of these embedding representations in two tensors of size (N, 4, d), T_{left} and T_{right} , where d is the embedding dimensionality. At this point, we merely employ a very simple distance measure on the embeddings to obtain the CMs of all pairwise puzzle pieces. Although the distance measure needs to be computed $16N^2$ times, the running time it takes is by far smaller than employing an NN-based CM the same number of times, which involves millions/billions of FLOPS (for each pair). In fact, the larger the puzzle is, the larger the speedup gain obtained over an NN-based CM, as will be demonstrated in Subsection 3.4.3.

3 Experimental Results

During our extensive experiments, we trained and evaluated the following three models: (1) Regular version of our novel TEN architecture, (2) ensemble version, TEN-Large, which contains four times as many parameters as TEN, and (3) pairwise, NN-based end-to-end (E2E) CM, as depicted in Figure 1(b). For the latter model, we used basically the same architecture presented schematically in Table 1, but instead of d outputs, this network outputs a single value, which indicates the degree of compatibility of a given pair of pieces. We have experimented intentionally with an NN-based model, as well, to study not only the actual speedup gain due to TEN during inference, but to assess the expected accuracy gap as a performance reference for future research. We trained all of the above networks with the same recipe, including an Adam optimizer [20], a learning rate of 1E-4 (with a decay factor of 0.9, in case the loss did not decrease for 5 epochs), a batch size of 64, and an epoch of 5000 iterations. To obtain the final results for TEN, TEN-Large, and NN-based E2E, we trained them over 600 epochs. TEN and TEN-Large were trained with *triplet-loss*, while the NN-based CM was trained with the *binary cross entropy loss* (labeling positive pairs as "0" and negative pairs as "1").

3.1 Datasets

To train our networks and evaluate them relatively to the classical CM methods, we used the DIV2K [21] dataset downscaled by a factor of 2 (due to bicubic interpolation). We chose this particular dataset to experiment with, since it has a sufficient amount of images for training and testing, and since the images are large enough for generating puzzles with 800-1000 pieces of size 28×28 pixels. Specifically, the training and validation subsets of DIV2K contain 800 and 100 high-quality images, respectively. In our experiments, we used 700 (of the 800 training images) to train TEN, TEN-Large, and the NN-based E2E CM. The remaining 100 images (from the training subset) were used as our held-out validation subset, and the DIV2K validation subset of 100 images was used as our test set. Next, we cropped each image into puzzle pieces of size 28×28 pixels, deleting the boundary pixels from each piece to generate an erosion effect of 13.8% (with respect to the piece size).

We chose to experiment with pieces of eroded boundaries, since this problem domain is a testbed for various practical, real-world JPPs (having to deal with damaged pieces around the edges). We generated only 1-pixel erosions, as this

Table 2: Dimensionality effect: d > 40 does not seem to gain higher Top-1 accuracy for both distance measures used, running TEN on half epochs (rather than on full training phase).

Distance Measure	Embedding Size - d			
Distance Measure	10	20	40	80
$1 - \cos ine$	31.1%	37.9%	40.7%	40.5%
Euclidean distance	46.3%	51.4%	54.4%	54.7%

minimal amount of degradation already resulted in poor CMs. (See Table 4 for specific results.) To evaluate the classical CMs on 1-pixel erosions, in a meaningful manner, we disposed the entire piece frame and considered only its remaining content (*i.e.*, if the original piece size is 28×28 pixels, then the eroded piece is of size 26×26 pixels). On the other hand, we retained the original piece size for all trainable CMs (*i.e.* TEN, TEN-Large, and NN-based E2E), such that each piece includes its eroded frame. Also, for the classical SSD, prediction-based, and L_1 CMs we made sure to represent the images in LAB color space (according to the specification of these methods), while using an RGB representation for all other CMs.

3.2 Dimensionality Effect

In general, the dimensionality of an embedding is one of its main characteristics. To determine practically the desired embedding dimensionality for an adequate representation of a piece edge e, we trained TEN on various dimensions, *i.e.* $d \in \{10, 20, 40, 80\}$. We stopped at d = 80, since TEN did not seem to yield better *Top-1 accuracy* on our test set, using a larger number of dimensions. (See exact definition of Top-1 accuracy in Subsection 3.4.1.) Indeed, empirical results consistently showed that using d = 40 was good enough, regardless of the distance measure used (see Table 2).

3.3 Distance Measure

Recall, to calculate the compatibility score between two embeddings z_l , z_r we have to use a distance function $D: \mathcal{Z} \times \mathcal{Z} \to \mathbb{R}$. Technically, D can be any desired function, including an NN-based one; however, to accelerate the computation as much as possible, we have focused on fast and simple distance measures.

• Cosine similarity: This embedding similarity is very common these days, in particular among the self-supervised learning field. Let z_l and z_r denote the embeddings obtained. Then the cosine similarity is given by

$$cosine(z_l, z_r) = \frac{z_l \cdot z_r}{\|z_l\| \|z_r\|}$$
(5)

In its raw form, the cosine projects all distances to be in the range [-1, 1], where the closest embeddings will get a score of 1 and vice versa. To force the cosine similarity to give a near-zero value to similar embeddings, we define

$$D(z_l, z_r) = 1 - cosine(z_l, z_r), \tag{6}$$

such that and all distances now lie in the range [0, 2].

• L_p Distance: This is a family of distance measures which differ from one another by the parameter p. In this work we examined three p values $\in \{1, 2, 3\}$, which correspond to the well-known L_1 , L_2 (Euclidean distance), and L_3 metrics. In general, the L_p distance between two embeddings is calculated according to

$$L_p(z_l, z_r) = \left(\sum_{i=1}^d |z_l[i] - z_r[i]|^p\right)^{1/p}$$
(7)

In all of the experiments, we trained our models with the above distance measures for d=40. A comparative performance is given in Table 3 with respect to Top-1 accuracy (see definition below). The results indicate that the L_p norm is preferable to the cosine similarity. More specifically, the best results were achieved using the L_2 Euclidean distance.

Table 3: Top-1 accuracies of our model (trained on half epochs) for 4 simple, fast distance measures and embedding size of 40; L_2 metric achieved highest score.

Distance Measure	Top-1 Accuracy
$1 - \cos$ ine	40.7%
L_1	51.8%
L_2 (Euclidean distance)	54.4%
L_3	54%

Table 4: Top-1 accuracies for different CMs: Our proposed embedding is more accurate than best classical CM tested by 8.3% and 11.4% for Type-1 and Type-2, respectively; NN-based E2E still yields highest rate.

Method	Type-1	Type-2
SSD	37%	29%
Prediction-based	46.4%	37.5%
L_1	52.3%	43.7%
MGC	56.3%	45.4%
TEN (ours)	59.4%	50.5%
TEN-Large (ours)	64.6%	56.8%
NN-based E2E	71.4%	64.1%

3.4 Performance Results

3.4.1 Top-1 Accuracy

Ideally, given an anchor piece edge, we would like an algorithm that assigns the best pairwise CM to the true adjacent edge among all other piece edges in the puzzle. The most common criterion to quantitatively assess the performance of any such CM procedure is the Top-1 classification rate.

We define a pair (z_a, z_p) of an (embedded) anchor edge and its (embedded) true adjacent edge to be Top-i compatible (with respect to a given CM procedure) if its computed CM is greater than the i-th computed CM between the (embedded) anchor edge and any (embedded) negative edge (z_a, z_n) , $\forall z_n \neq z_a, z_p$. Ideally, Top-1 should approach 100% accuracy for a perfect CM module. Practically, the higher it is, the more accurate the CM computation.

We computed Top-1 accuracies on the entire test set of 100 puzzles, each containing 800-1000 pieces. As the results indicate, NN-based E2E performs best, for now, with Top-1 accuracies of 71.4% and 64.1% for type-1 and type-2, respectively. Our TEN-Large yields, though, second-best CM scores with Top-1 accuracies of 64.6% and 56.8% for Type-1 and Type-2, respectively. This gap might be attributed to the intuitive insight that an NN-based model "sees" an entire pair before assessing the extent of compatibility between the two pieces. In contrast, the twin models f_{left} and f_{right} try to predict, essentially, each other's embedding, which is a harder task.

3.4.2 Black-Box Reconstruction

Another way to conduct a comparative performance evaluation is to supplement each CM module with the same reconstruction algorithm, and test which CM, coupled with this reconstruction "black box", contributes the most to the reassembled puzzle. We chose Gallagher's reconstruction algorithm as a "reference" black box, since its code is publicly available and is commonly used in many other studies. To determine how successful the reconstruction is, we apply the *neighbor accuracy* criterion, which is already incorporated into Gallagher's code. We experimented with all of the traditional CMs, as well as our newly proposed TEN and TEN-Large, and recorded the average neighbor accuracy (over the 100 test images) obtained for each method after employing Gallagher's reconstruction. Note that the uniform reconstruction was employed merely for an additional comparative evaluation, *i.e.* the key point here is not necessarily the absolute neighbor accuracy obtained, but rather the significant improvement of a novel CM model, relatively to the various traditional measures. Although other reconstruction algorithms may well achieve better accuracy results, investigating their relative contribution is beyond the scope of this paper.

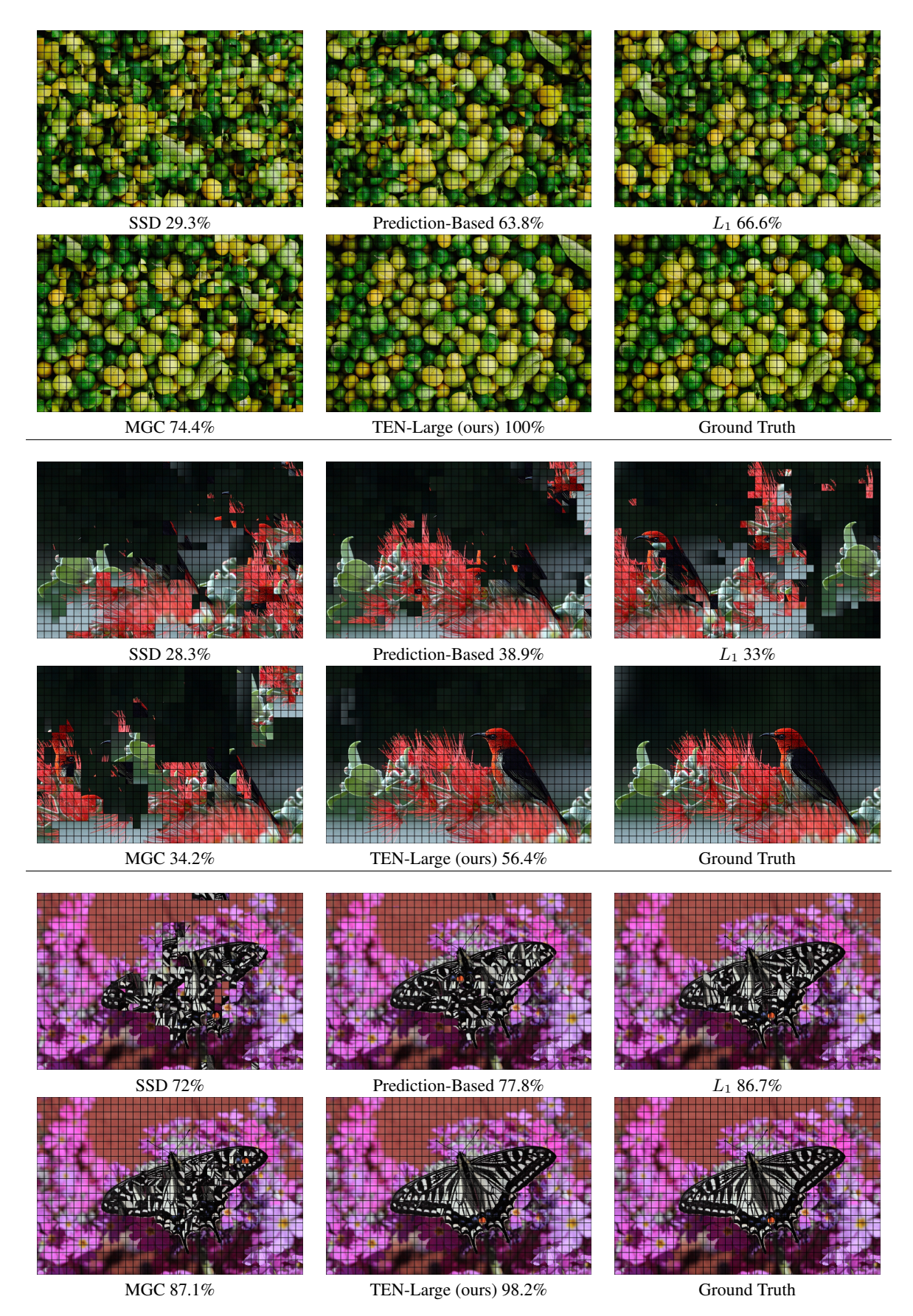


Figure 2: Sample of black-box reconstructions for Type-1 variant; our proposed CM exhibits superior performance to that of classical methods. 8

Table 5: Comparative reconstruction rates due to evaluated CMs + black box; proposed architecture(s) yield superior neighbor accuracy (for both Type-1 and Type-2) compared to classical methods.

Type-1

Method	Neighbor Accuracy	Perfect
SSD	25.04%	0
Prediction-based	39.96%	0
L_1	44.38%	1
MGC	45.81%	1
TEN (ours)	52.89%	0
TEN-Large (ours)	60.68%	5
NN-based E2E	75.27%	11

Type-2

Method	Neighbor Accuracy	Perfect
SSD	6.97%	0
Prediction-based	13.16%	0
L_1	16.22%	0
MGC	16.45%	0
TEN (ours)	21.83%	0
TEN-Large (ours)	30.24%	0
NN-based E2E	45.07%	1

The neighbor accuracy results (for the evaluated CMs, coupled with the reconstruction black box) are summarized in Table 5 for both Type-1 and Type-2 variants. As can be seen, using TEN-Large resulted in an average reconstruction increase of 14.9% and 13.8%, respectively, for Type-1 and Type-2, over the best known CM due to MGC.

A visual reconstruction comparison between the classical CM's and our best proposed model, TEN-Large, is shown in Figure 2 on a few selected images.

3.4.3 Inference Times

Table 6 gives the actual running times for computing all of the $16N^2$ combinations of a single puzzle with N pieces, on average. We experimented with $N \in \{100, 200, 400, 800, 1600, 3200\}$, i.e. with a growing number of pieces, to underscore the impact of our novel architecture compared to the NN-based (E2E) method. The running times due to the embedding approach (of TEN and TEN-Large) include the time to compute the final distance measures for all combinations.

Note the speedup gain as a function of puzzle size. Specifically, TEN/TEN-Large run 454/176 times faster than the NN-based model employed on 100-piece puzzles. Moreover, our TEN/TEN-Large models become 2771/1657 times faster than E2E on puzzles with 3200 pieces, which makes TEN the fastest known NN-based CM module. Figure 3 visualizes how fast our TEN and TEN-Large scheme compare to the NN-based (E2E) approach.

Also, note that GPU/CPU utilization along with other factors like code optimization can cause changes in inference times as reported in Table 6. The reported inference times were measured on a modern PC with 3.5GHz CPU, 32GB RAM, and a single GPU with 11GB memory.

4 Conclusions

In this paper we presented the novel framework, Twin Embedding (Neural) Networks (TEN), for computing very efficiently, yet fairly accurately, CMs for real-world JPP applications. The proposed embedding approach achieves a significant improvement in Top-1 accuracy compared to the classical CMs evaluated. This innovation resulted also in an enhanced reconstruction of puzzles with eroded boundaries, as was demonstrated by the comparison between different CMs coupled with the same black-box reconstruction. We have focused deliberately on a problem domain with such

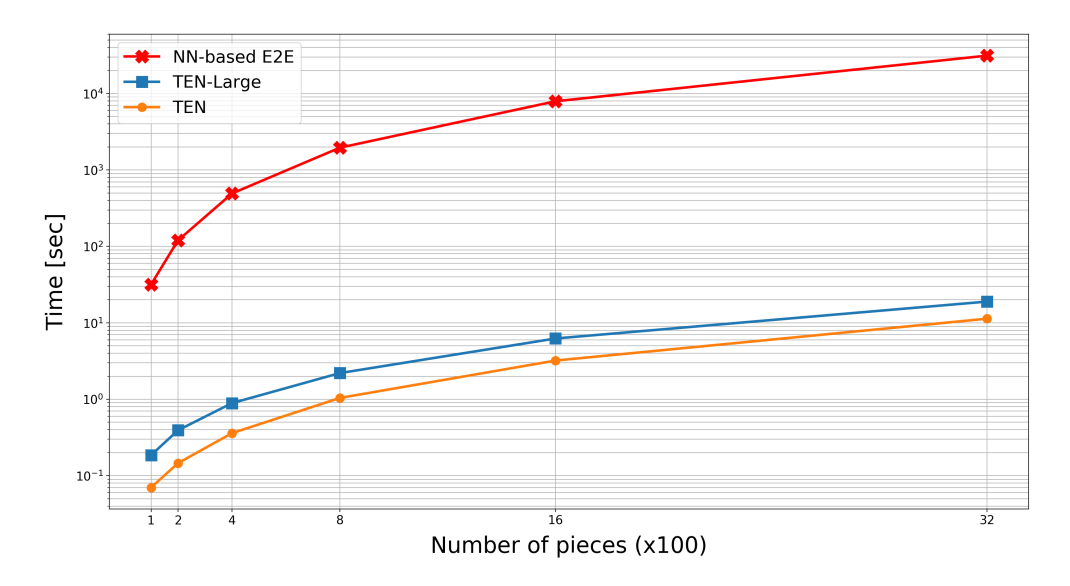


Figure 3: Comparative inference times of our new embedding-based CMs, TEN and TEN-Large, versus NN-based (E2E); computation time is dramatically reduced for $16N^2$ pairwise piece compatibilities.

Table 6: Wall-clock inference times of our proposed embedding approach compared to (E2E) NN-based; TEN (and TEN-Large) boost inference speed by orders of magnitude as more pieces are added to puzzle.

# Pieces	TEN	TEN-Large	E2E
100	0.07 sec	0.18 sec	31.8 sec
200	0.14 sec	0.39 sec	2 min
400	0.36 sec	0.89 sec	8.2 min
800	1 sec	2.2 sec	32.6 min
1600	3.2 sec	6.2 sec	2.2 hours
3200	11.3 sec	18.9 sec	8.7 hours

degraded puzzles, unlike most JPP works which deal typically with synthetic perfect puzzles, since it involves a useful testbed for real-world scenarios, where puzzle pieces undergo severe degradation along the edges.

We believe that our novel embedding paradigm could also affect significantly the accelerated research and development of further JPPs containing (tens of) thousands of eroded pieces for highly challenging problems, without compromising much on inference speed, as opposed to computationally-intensive NN-based CM models which run slower by a few orders of magnitude.

Indeed, NN-based E2E models are relatively more accurate, for now, but we intend to address this limitation of our novel framework, as part of future work, to further close the accuracy gap while maintaining fast running times. We have already been exploring to that effect enhanced architectures (due to additional ensembles, additional CNN layers, different inputs than RGB, etc.) and additional loss functions, like the *contrastive loss function* and others. Moreover, given the inherent redundancy between the f_{left} and f_{right} networks, in view of the same tasks performed by both models, albeit with respect to different edges, we intend to draw on this insight to derive a unified model for extracting bi-directional embeddings for a given piece. Finally, we will also attempt to explore the underlying meaning of our model's embedding.

References

- [1] T. S. Cho, S. Avidan, and W. T. Freeman. A probabilistic image jigsaw puzzle solver. In *Proceedings of the IEEE Conference on Computer Vision and Pattern Recognition*, pages 183–190, 2010.
- [2] D. Pomeranz, M. Shemesh, and O. Ben-Shahar. A fully automated greedy square jigsaw puzzle solver. In *Proceedings of the IEEE Conference on Computer Vision and Pattern Recognition*, pages 9–16, 2011.
- [3] G. Paikin and A. Tal. Solving multiple square jigsaw puzzles with missing pieces. In *Proceedings of the IEEE Conference on Computer Vision and Pattern Recognition*, pages 4832–4839, 2015.
- [4] A. C. Gallagher. Jigsaw puzzles with pieces of unknown orientation. In *Proceedings of the IEEE Conference on Computer Vision and Pattern Recognition*, pages 382–389, 2012.
- [5] K. Son, J. Hays, and D. B. Cooper. Solving square jigsaw puzzles with loop constraints. In *Proceedings of the European Conference on Computer Vision*, pages 32–46. Springer, 2014.
- [6] R. Yu, C. Russell, and L. Agapito. Solving jigsaw puzzles with linear programming. In *Proceedings of The British Machine Vision Conference*, pages 139.1–139.12, 2016.
- [7] S. Kilho, D. Moreno, J. Hays, and D. B. Cooper. Solving square jigsaw puzzle by hierarchical loop constraints. *IEEE Transactions on Pattern Analysis and Machine Intelligence*, pages 2222–2235, 2019.
- [8] D. Mondal, Y. Wang, and S. Durocher. Robust solvers for square jigsaw puzzles. In *Proceedings of the International Conference on Computer and Robot Vision*, pages 249–256, 2013.
- [9] T. M. Paixao, R. F. Berriel, M. C. Boeres, C. Badue, A. F. De Souza, and T. Oliveira-Santos. A deep learning-based compatibility score for reconstruction of strip-shredded text documents. In *Proceedings of the IEEE 31st SIBGRAPI Conference on Graphics, Patterns and Images*, pages 87–94, 2018.
- [10] N. I. Forrest, H. Song, W.M. Matthew, A. Khalid, J.D. William, and K. Kurt. Squeezenet: AlexNet-level accuracy with 50x fewer parameters and <0.5MB model size. *arXiv*:1602.07360, 2015.
- [11] D. Rika, D. Sholomon, O. E. David, and N. S. Netanyahu. A novel hybrid scheme using genetic algorithms and deep learning for the reconstruction of Portuguese tile panels. In *Proceedings of the ACM Conference on Genetic and Evolutionary Computation*, pages 1319–1327, 2019.
- [12] D. Bridger, D. Danon, and A. Tal. Solving jigsaw puzzles with eroded boundaries. In *Proceedings of the IEEE Conference on Computer Vision and Pattern Recognition*, pages 3526–3535, 2020.
- [13] P. Isola, J. Zhu, T. Zhou, and A. A. Efros. Image-to-image translation with conditional adversarial networks. In *Proceedings of the IEEE Conference on Computer Vision and Pattern Recognition*, 2017.
- [14] O. Ronneberger, P. Fischer, and T. Brox. U-Net: Convolutional networks for biomedical image segmentation. *arXiv:1505.04597*, 2016.
- [15] Marie-Morgane Paumard, David Picard, and Hedi Tabia. Deepzzle: Solving visual jigsaw puzzles with deep learning and shortest path optimization. *IEEE Transactions on Image Processing*, 29:3569–3581, 2020.
- [16] Ru Li, Shuaicheng Liu, Guangfu Wang, Guanghui Liu, and Bing Zeng. JigsawGAN: Auxiliary learning for solving jigsaw puzzles with generative adversarial networks. *IEEE Transactions on Image Processing*, 31:513–524, 2022.
- [17] J. Nagi, F. Ducatelle, G.A. Di Caro, D. Cireşan, U. Meier, A. Giusti, F. Nagi, J. Schmidhuber, and L.M. Gambardella. Max-pooling convolutional neural networks for vision-based hand gesture recognition. In *Proceedings of the IEEE International Conference on Signal and Image Processing Applications*, pages 342–347, 2011.
- [18] V. Nair and G.E. Hinton. Rectified linear units improve restricted boltzmann machines. In *Proceedings of the 27th International Conference on Machine Learning*, pages 807–814, 2010.
- [19] F. Schroff, D. Kalenichenko, and J. Philbin. FaceNet: A unified embedding for face recognition and clustering. In *Proceedings of the IEEE Conference on Computer Vision and Pattern Recognitio*, pages 815–823, 2015.
- [20] D. P. Kingma and J. Ba. Adam: A method for stochastic optimization. arXiv:1412.6980, 2017.
- [21] E. Agustsson and R. Timofte. NTIRE 2017 challenge on single image super-resolution: Dataset and study. In *Proceedings of the IEEE Conference on Computer Vision and Pattern Recognition Workshops*, July 2017.